Vibrational spectroscopic investigation and conformational analysis of 1-heptylamine: A comparative density functional study

ARTICLE *in* SPECTROCHIMICA ACTA PART A MOLECULAR AND BIOMOLECULAR SPECTROSCOPY · JUNE 2013

Impact Factor: 2.35 · DOI: 10.1016/j.saa.2013.05.097 · Source: PubMed

4 AUTHORS, INCLUDING:

Mahir Tursun
Dumlupinar Üniversitesi
18 PUBLICATIONS **35** CITATIONS
SEE PROFILE

Gürkan Keşan
University of South Bohemia in České Bud…
19 PUBLICATIONS **67** CITATIONS
SEE PROFILE

Spectrochimica Acta Part A: Molecular and Biomolecular Spectroscopy 114 (2013) 668–680

Contents lists available at SciVerse ScienceDirect

Spectrochimica Acta Part A: Molecular and Biomolecular Spectroscopy

journal homepage: www.elsevier.com/locate/saa

Vibrational spectroscopic investigation and conformational analysis of 1-heptylamine: A comparative density functional study

Mahir Tursun [a], Gürkan Keşan [b], Cemal Parlak [a,*], Mustafa Şenyel [c]

[a] Department of Physics, Dumlupınar University, Kütahya 43100, Turkey
[b] Institute of Physics and Biophysics, Faculty of Science, University of South Bohemia, Branišovská 31, České Budějovice 370 05, Czech Republic
[c] Department of Physics, Science Faculty, Anadolu University, Eskişehir 26470, Turkey

HIGHLIGHTS

- Infrared, Raman and quantum chemical calculations of 1-ha.
- The TT isomer is supposed to be the most stable form of 1-ha.
- Conformational energy barriers are low and independent of the solvent.
- Vibrational frequencies and intensities change when going from non-polar to polar solvents.

GRAPHICAL ABSTRACT

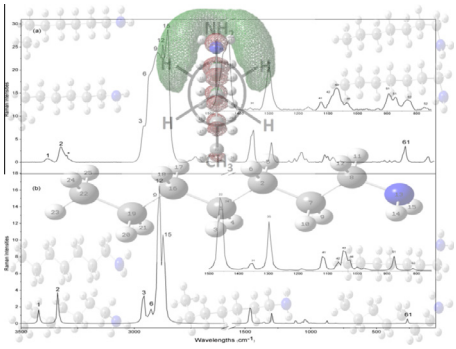

ARTICLE INFO

Article history:
Received 16 April 2013
Received in revised form 16 May 2013
Accepted 24 May 2013
Available online 4 June 2013

Keywords:
1-Heptylamine
Vibrational spectra
DFT
PED

ABSTRACT

FT-IR and Raman spectra of 1-heptylamine (1-ha) have been recorded in the region of 4000–10 cm^{-1} and 4000–50 cm^{-1}, respectively. The conformational analysis, optimized geometric parameters, normal mode frequencies and corresponding vibrational assignments of 1-ha ($C_7H_{17}N$) have been examined by means of the Becke-3-Lee-Yang-Parr (B3LYP) density functional theory (DFT) method together with the 6-31++G(d,p) basis set. Furthermore, reliable vibrational assignments have been made on the basis of potential energy distribution (PED) and the thermodynamics functions, highest occupied and lowest unoccupied molecular orbitals (HOMO and LUMO) of 1-ha have been predicted. Calculations have been carried out with the possible ten conformational isomers (TT, TG, GT, GT_1, GG_1, GG_2, GG_3, GG_4, GG_5, GG_6; T and G denote trans and gauge) of 1-ha, both in gas phase and in solution. Solvent effects have theoretically been investigated using benzene and methanol. All results indicate that the B3LYP method provides satisfactory evidence for the prediction of vibrational frequencies and the TT isomer is the most stable form of 1-ha.

Introduction

1-Heptylamine, called in the literature by different names such as 1-aminoheptane and 1-heptanamine, is a linear aliphatic amine and very versatile molecule. It has been the subject of many scientific studies. For example, 1-ha has been used in synthesizing hybrid biomaterials [1], fluorescent tocopherols [2], lithium dialkylamides [3], amine complexes of the cyclopentadienyliron dicarbonyl complex cation [4,5], new oxaanalogues of spermine [6], zirconium benzylamino-N,N-dimethylphosphonate phosphate materials [7], (2*R*,3*R*,4*S*)-4,7-diamino-2,3-dihydroxy heptanoic acid [8], the heptylamine adduct of benzylidenemalononitrile [9] and naphthanilide-containing organogelator [10].

1-ha has also been employed in the researching the magnetic properties of FePt nanoparticles [11], the influence of

* Corresponding author. Tel.: +90 274 265 20 31x3116; fax: +90 274 265 20 14.
E-mail address: cparlak@dpu.edu.tr (C. Parlak).

1386-1425/$ - see front matter © 2013 Elsevier B.V. All rights reserved.
http://dx.doi.org/10.1016/j.saa.2013.05.097

nanostructured materials on biointerfacial interactions [12], the underivatized biogenic amines in human urine [13], the aliphatic amines in natural surface water and wastewater [14], chemicals inducing acute irritant contact dermatitis [15], different alkanoic acid–alkylamine complexes [16,17], anti-tarnish coatings [18], piezoelectric quartz crystal microbalances sensors [19], protein deposition through binary monolayer colloidal crystals [20], plasma polymerization of amine-containing thin films [21,22], controlled growth and modification of vertically-aligned carbon nanotubes [23] and sensitive amperometric biosensors [24].

Vibrational spectroscopy has widely been used as the standard tool for structural characterization of molecular systems together with DFT calculations. DFT is popular as it is a cost-effective procedure for studying the physical properties of molecules. Unlike the Hartree Fock (HF) theory, DFT recovers electron correlation in the self-consistent Kohn–Sham procedure through the functions of electron density. The DFT/B3LYP model exhibits good performance on electron affinities, excellent performance on bond energies and reasonably good performance on vibrational frequencies and geometries of organic compounds [25–32].

There are ample examples of 1-ha being used as an intermediate product in the literature. However, though 1-ha has wide applications in many areas of science, to the best of our knowledge, there is no detailed information present in the literature about its vibrational spectroscopic properties. A detailed, quantum chemical study will aid in making definitive assignments to the fundamental normal modes and in clarifying the obtained experimental data of 1-ha. Furthermore, all data presented as theoretically and experimentally may be helpful in the context of the further studies. For the above goals, we have reported vibrational spectra of 1-ha. The vibrational frequencies with PED values, HOMO and LUMO data and conformational analysis of 1-ha are investigated by means of the B3LYP/6-31++G(d,p) level. The results of the theoretical and spectroscopic studies are here reported.

Experimental

A commercially available sample of 1-ha was purchased from Aldrich (99%) and used without further purification. FT-MIR and FT-FIR spectra of 1-ha were recorded in the region of 4000–400 cm^{-1} and 400–10 cm^{-1} with Bruker Optics IFS66v/s FTIR spectrometer at a resolution of 2 cm^{-1}. Raman spectrum was obtained using a Bruker Senterra Dispersive Raman microscope spectrometer with 532 nm excitation from a 3B diode laser having 2 cm^{-1} resolution in the spectral region of 4000–50 cm^{-1}. All spectra are normally carried out in a liquid phase of 1-ha.

Computational details

All the calculations were performed using Gaussian 09W program package [33] and GaussView 5.0.8 [34] was used for visualization of the structure and simulated vibrational spectra. Many possible isomers could be proposed for 1-ha; however, comparison with previously reported studies [35,36] reduced the number of possible stable conformers to 10: TT, TG, GT, GT_1, GG_1, GG_2, GG_3, GG_4, GG_5 and GG_6 isomers (Fig. 1). The Newman projections of the isomers investigated are along the C1–C2, C7–C8 and C16–C19 planes and C19–C22, C7–C8 and C8–N13 bonds (Fig. 1). For these calculations, 10 forms of 1-ha were first optimized by B3LYP level of theory using 6-31++G(d,p) basis set both in the gas phase and in benzene and methanol solvent environments. After the optimization, harmonic vibrational frequencies and corresponding vibrational intensities for ten isomers of 1-ha were calculated by using the same method and basis set and then scaled by 0.955 (above 1800 cm^{-1}) and 0.977 (under 1800 cm^{-1}) [31,32]. PED calculations, which show the relative contributions of the redundant internal coordinates to each normal vibrational mode of the molecule and thus make it possible to describe the character of each mode numerically, were carried out by the VEDA 4 (Vibrational Energy Distribution Analysis) [37]. Calculated Raman activities were converted to relative Raman intensities (I_R) using the following relationship derived from the intensity theory of Raman scattering [31,38]:

$$I_i = f(v_0 - v_i)^4 S_i / v_i[1 - \exp(-hcv_i/kT)]$$

where v_0 is the laser exciting wavenumbers in cm^{-1}, v_i is the vibrational wavenumbers of the ith normal mode, S_i is the Raman scattering activity of the normal mode v_i and f is a suitably chosen common normalization factor for all peak intensities, 10^{-14}. h, k, c and T are Planck and Boltzmann constants, speed of light and temperature in Kelvin, respectively.

Results and discussion

Geometrical structures

To clarify vibrational frequencies it is essential to examine the geometry of the compound, as small changes in geometry can cause substantial changes in frequencies. Gibbs free energy of the optimized geometries in gas phase and in solution of ten forms of 1-ha with B3LYP/6-31++G(d,p) method are given in Table 1. Regarding the calculated free energies for gas phase, the TT isomer is more stable than TG, GT, GT_1, GG_1, GG_2, GG_3, GG_4, GG_5 and GG_6 by 0.064, 0.77, 0.22, 0.77, 0.92, 0.37, 0.33, 0.33 and 0.37 kcal/mol, respectively. Possible interconversion between any two conformers, except for TT, has a lower energy barrier. Low interconversion energy barriers obtained for 1-ha suggest that interconversions are likely to happen at room temperature [39–40]. According to the calculations for mole fractions of individual conformers [28–32], 1-ha in the gas phase prefers TT, TG, GT_1 and GG_3, GG_4, GG_5, GG_6 forms with preferences of 18%, 16%, 12% and 10%, respectively. GT, GG_1 and GG_2 isomers have the lowest relative abundance with preferences of 5% and 4%, respectively. Similarly, the calculated free energies in benzene as a non-polar solvent show that the TT form is more stable than other forms and that 1-ha prefers TT, TG, GT_1, GG_4/GG_5, GT, GG_3/GG_6, GG_1 and GG_2 forms with preferences of 26%, 17%, 14%, 8%, 7%, 6%, 5% and 4%, respectively. The calculated free energies in methanol, as a polar solvent, also show that the TT form is more stable than the other forms and 1-ha prefers TT, TG, GT_1, GG_4/GG_5, GT/GG_3/GG_6 and GG_1/GG_2 forms with preferences of 23%, 17%, 15%, 9%, 6% and 4%, respectively.

Several thermodynamics parameters (capacity, zero point energy, entropy, etc.) calculated by B3LYP/6-31++G(d,p) for TT isomer are presented in Table 1. The variation in the zero point vibrational energy seems to be insignificant. The total energy and change in total entropy of 1-ha are at room temperature. The dipole moment is expected to be larger in solution than the corresponding dipole moment in the gas phase. This situation is clearly observed in Table 1. The dipole moment increases gradually from a lower to a higher dielectric and the increases going from gas to non-polar/polar solvents are about 13%/30%.

Some of the optimized geometric parameters (bond lengths, bond and dihedral angles) calculated by B3LYP/6-31++G(d,p) are listed in Table 2. To the best of our knowledge, the experimental data on geometric structure of 1-ha is not available in the literature. Therefore, the theoretical results for the TT isomer of 1-ha have been compared together with the data of related parts of 5,7-diamino-1-heptylpyrimido[4,5-*d*]pyrimidine-2,4(1*H*,3*H*)-dione [41] and 7-aminoheptylazanium iodide [42] as given in Table 2.

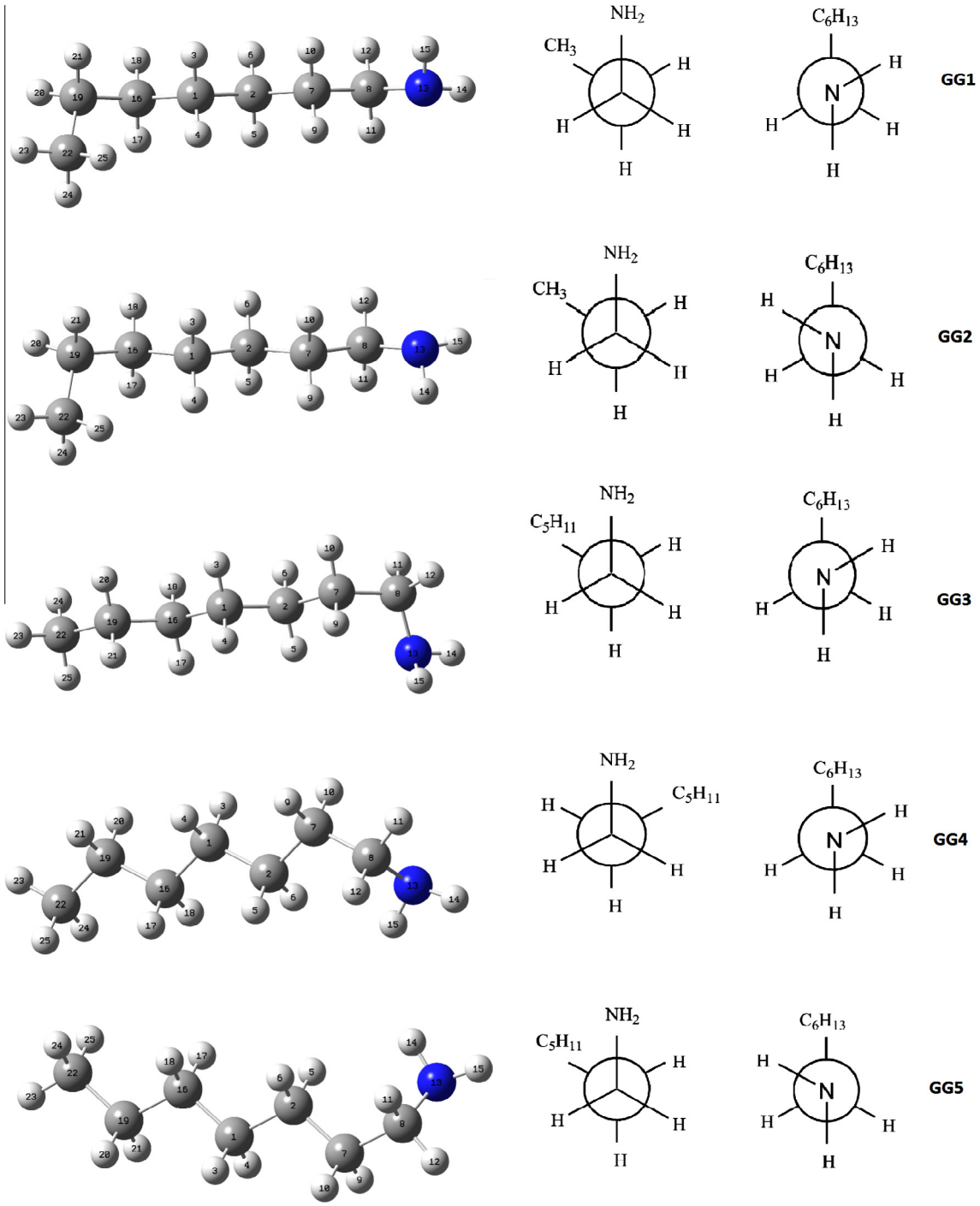

Fig. 1. Possible optimized structures and Newman projections of ten isomers of 1-ha.

Theoretically calculated structural data for 1-ha are consistent with previously reported structural data for its fragments [41–42].

Generally, it is expected that the bond distances calculated by electron-correlated methods are longer than the experimental distance. This situation is observed in Table 2, as expected. Overall, the calculated bond lengths are in good agreement with experimental results. The mean absolute deviation (MAD) of bond lengths of the TT form for all medium is about 0.083 Å. The biggest difference between the experimental and calculated bond distances for gas phase, benzene and methanol is 0.140, 0.141, 0.141 Å. The observed differences in bond distances are not due to the theoretical shortcomings, as experimental results are also subject to variations owing to the insufficient data to calculate the equilibrium structure and which are sometimes averaged over zero point vibrational motion. In X-ray structure the error in the position of the hydrogen atoms is such that their bonding parameters greatly vary compared to the non-hydrogen atoms. Intra- or intermolecular hydrogen bonding is also an important factor in the crystalline state of the compound.

As can be seen in Table 2, the biggest difference between the experimental and calculated bond angels belongs to C8–N13–H14 angel at about 7.6° for the TT form. All the other bond angles

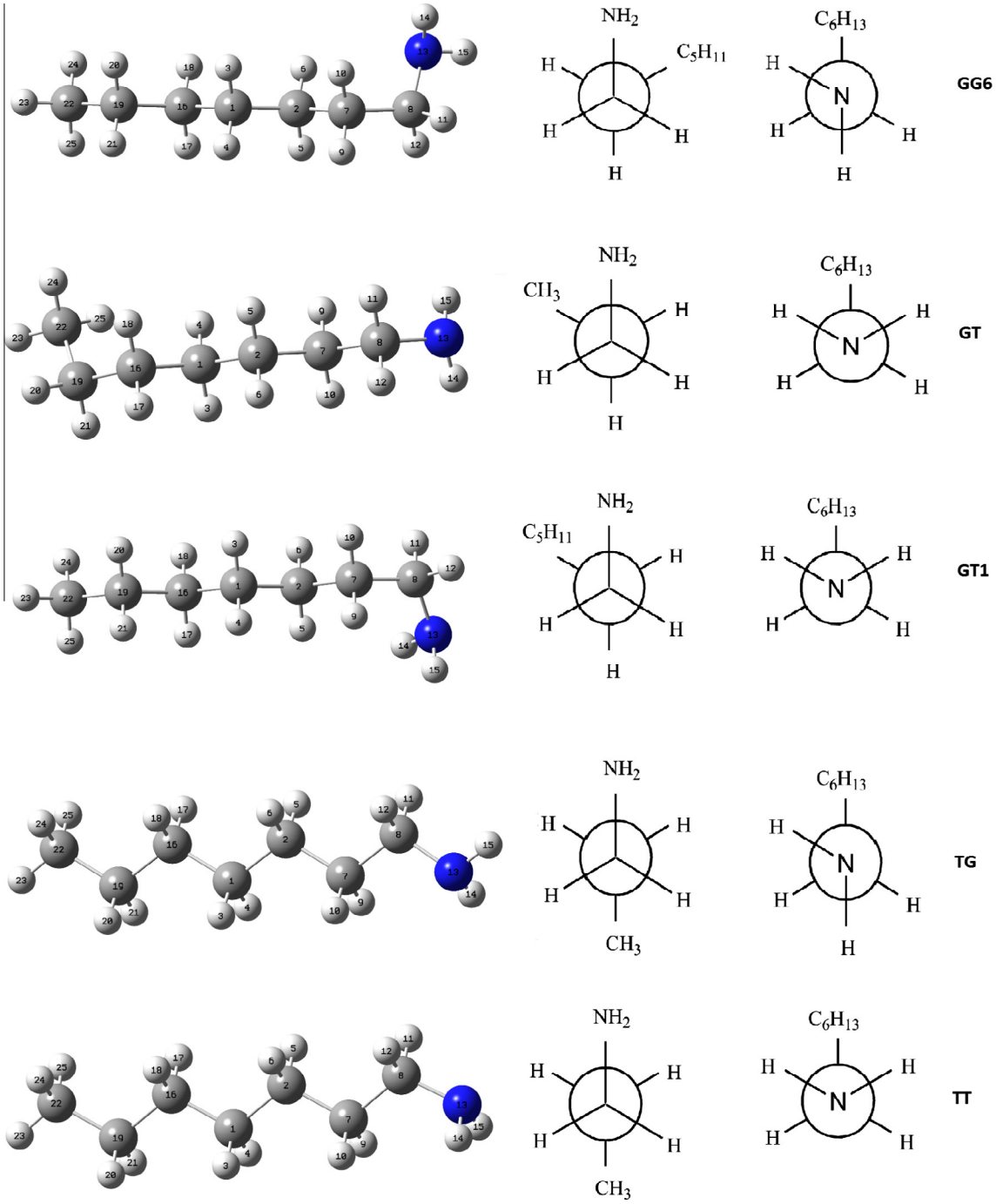

Fig. 1 (*continued*)

are reasonably close to the experimental data. The MAD values of calculated bond angles of the TT form for gas phase, benzene and methanol are 1.23°, 1.20° and 1.19°, respectively. Some changes, as seen in Table 2, are also observed in the dihedral angles. Among all dihedral angles, the largest deviation is observed for C2–C1–C16–C19 at about 3.0°. The MAD value of calculated dihedral angles of TT form for gas phase, benzene and methanol are 2.02°, 2.21° and 2.02°, respectively.

Vibrational studies of 1-ha

To the best of our knowledge, the vibrational assignments for 1-ha in the middle and far infrared regions of the spectrum have not been reported in the literature. All experimental and theoretical vibrational frequencies for the TT isomer of 1-ha, along with corresponding vibrational assignments and intensities, are given in Tables 3–5 and Figs. 2–4. The vibrational frequencies for the complete set of conformations investigated are available as Supplementary material (Tables S1–6, Fig. S1). All calculated frequency values presented in this paper are obtained within the harmonic approximation. This allows us to describe vibrational motion in terms of independent vibrational modes, each of which is governed by a simple one-dimensional harmonic potential. The 1-ha molecule consists of 25 atoms, having 69 normal vibrational modes, and it belongs to the point group C_1 with only identity (E) symmetry element or operation. It is very difficult to determine the vibra-

Table 1
Some features in various medium for different conformations of 1-ha.

Geometry	Optimized energy (Hatree)			Feature [B3LYP/6-31++G(d,p)]	Gas	Benzene	Methanol
	Gas phase	C_6H_6	CH_3OH		TT		
GG_1	−331.580305	−331.582374	−331.585370	Molar volume (cm^3/mol)	126.68		
GG_2	−331.580072	−331.582261	−331.585348	Recommend (a_0)	4.56		
GG_3	−331.580947	−331.582723	−331.585565	Dipole moment (Debye)	1.53	1.73	2.00
GG_4	−331.581008	−331.583040	−331.585938	Thermal total energy (kcal/mol)	154.33	154.29	154.11
GG_5	−331.581010	−331.583040	−331.585938	Heat capacity (kcal/mol K)	38.69	38.70	38.68
GG_6	−331.580945	−331.582723	−331.585565	Entropy (kcal/mol K)	102.6	102.7	102.7
GT_1	−331.581187	−331.583483	−331.586435	Vibrational energy (kcal/mol)	152.55	152.46	152.34
GT	−331.580315	−331.582661	−331.585760	Zero point vibrational energy (kcal/mol)	147.44	147.34	147.21
TG	−331.581433	−331.583615	−331.586643				
TT	−331.581535	−331.583924	−331.587008				

Table 2
Optimized geometric parameters for TT form of 1-ha in various medium.

Bond lengths (Å)	Exp.[a]	TT/B3LYP/6-31++G(d,p)			Bond/dihedral angles (°)	Exp.[a]	TT/B3LYP/6-31++G(d,p)		
		Gas	Benzene	Methanol			Gas	Benzene	Methanol
C1–C2	1.523	1.535	1.535	1.535	C2–C7–H9	109.0	109.5	109.2	109.5
C1–H3	0.990	1.100	1.100	1.100	C2–C7–H10	109.0	109.5	110.0	109.5
C1–H4	0.990	1.100	1.100	1.100	C8–C7–H9	109.0	109.0	109.0	108.9
C1–C16	1.518	1.534	1.534	1.535	C8–C7–H10	109.0	109.0	108.6	108.9
C2–H5	0.990	1.100	1.100	1.100	H9–C7–H10	107.8	106.2	106.4	106.5
C2–H6	0.990	1.100	1.100	1.100	C7–C8–H11	109.1	109.4	109.0	109.4
C2–C7	1.527	1.535	1.534	1.535	C7–C8–H12	109.1	109.4	109.3	109.4
C7–C8	1.520	1.538	1.530	1.536	C7–C8–N13	112.3	116.4	111.0	115.9
C7–H9	0.990	1.100	1.100	1.100	H11–C8–H12	107.9	106.1	106.7	106.4
C7–H10	0.990	1.100	1.098	1.100	H11–C8–N13	109.1	107.5	113.1	107.7
C8–H11	0.990	1.098	1.104	1.098	H12–C8–N13	109.1	107.5	107.6	107.7
C8–H12	0.990	1.098	1.097	1.098	C8–N13–H14	118.0[b]	110.9	110.3	109.9
C8–N13	1.478	1.466	1.471	1.472	C8–N13–H15	112.0[b]	110.9	110.7	109.9
N13–H14	0.877[b]	1.017	1.018	1.018	H14–N13–H15	103.0[b]	107.1	106.7	106.1
N13–H15	0.898[b]	1.017	1.017	1.018	C1–C16–H17	109.0	109.3	109.3	109.2
C16–H17	0.990	1.100	1.100	1.100	C1–C16–H18	109.0	109.3	109.3	109.2
C16–H18	0.990	1.100	1.100	1.100	C1–C16–C19	113.0	113.7	113.7	113.7
C16–C19	1.524	1.535	1.535	1.535	H17–C16–H18	107.8	106.0	106.1	106.2
C19–H21	0.990	1.099	1.099	1.099	H17–C16–C19	109.0	109.1	109.1	109.1
C19–H20	0.990	1.099	1.099	1.099	H18–C16–C19	109.0	109.1	109.1	109.1
C19–C22	1.529	1.533	1.533	1.533	C16–C19–H21	108.8	109.2	109.2	109.2
C22–H23	0.980	1.095	1.096	1.096	C16–C19–H20	107.8	109.2	109.2	109.2
C22–H24	0.980	1.097	1.097	1.097	C16–C19–C22	113.7	113.3	113.3	113.3
C22–H25	0.980	1.097	1.097	1.097	H21–C19–H20	107.7	106.1	106.1	106.2
Bond angels (°)					H21–C19–C22	108.8	109.4	109.4	109.4
					H20–C19–C22	108.8	109.4	109.4	109.4
C2–C1–H3	108.3	109.2	109.2	109.2	C19–C22–H23	109.5	111.4	111.4	111.4
C2–C1–H4	108.3	109.2	109.2	109.2	C19–C22–H24	109.5	111.2	111.1	111.1
C2–C1–C16	116.0	113.6	113.6	113.6	C19–C22–H25	109.5	111.2	111.1	111.1
H3–C1–H4	107.4	106.0	106.1	106.2	H23–C22–H24	109.5	107.7	107.7	107.7
H3–C1–C16	108.3	109.2	109.2	109.2	H23–C22–H25	109.5	107.7	107.7	107.7
H4–C1–C16	108.3	109.2	109.2	109.2	H24–C22–H25	109.5	107.5	107.5	107.6
C1–C2–H5	109.1	109.2	109.2	109.2	C16–C1–C2–C7	178.8[b]	180.0	179.9	180.0
C1–C2–H6	109.1	109.2	109.1	109.2	C2–C1–C16–C19	−177.0[b]	−180.0	180.0	−180.0
C1–C2–C7	112.5	113.7	113.4	113.6	C1–C2–C7–C8	−178.7[b]	−180.0	179.9	−180.0
H5–C2–H6	107.8	106.0	106.1	106.2	C2–C7–C8–N13	−177.8[b]	180.0	179.1	180.0
H5–C2–C7	109.1	109.2	109.5	109.2	C1–C16–C19–C22	177.6[b]	−180.0	−179.9	−180.0

[a] 5,7-Diamino-1-heptylpyrimido[4,5-*d*]pyrimidine-2,4(1*H*,3*H*)-dione [41].
[b] 7-Aminoheptylazanium iodide [42].

tional assignments of 1-ha due to its low symmetry and at least 10 possible conformers. Therefore, some modes include the combination of several vibrational bands arising from possible isomers of 1-ha and the assignments of vibrational modes have been provided by VEDA 4. The following are some of the important vibrational motions observed.

NH_2 stretching

According to the amine functional groups, NH_2 antisymmetric and symmetric stretching vibrations (dilute solution spectra) are observed between 3550–3330 cm^{-1} and 3450–3250 cm^{-1}, respectively [43]. In the present study, NH_2 antisymmetric and symmetric stretching vibrations of 1-ha have been observed at 3371 cm^{-1} (IR), 3385 cm^{-1} (R) and 3289 cm^{-1} (IR), 3325 cm^{-1} (R), respectively. The NH_2 stretching fundamentals are also consistent with those previously reported for heptylamine-containing complexes [4,5], where these modes have been observed in the range 3313–3265 cm^{-1} (IR). NH_2 antisymmetric and symmetric modes for gas phase have been calculated as 3422 cm^{-1} (TT, GT), 3427 cm^{-1} (TG, GG_1 and GG_2), 3431 cm^{-1} (GT_1), 3428 cm^{-1} (GG_3,

Table 3
Calculated vibrational frequencies (cm^{-1}) for TT form of 1-ha in gas phase.

Mode	Assignments	Experimental		B3LYP/6-31++G(d,p)			
				Gas Phase			
	PED[a] (⩾10%)	IR	Raman	ν[b]	ν[c]	I_{IR}[d]	I_R[d]
ν_1	νNH(100)	3371	3385	3583	3422	0.28	7.58
ν_2	νNH(99)	3289	3325	3495	3338	1.96	17.76
ν_3	νCH(95)		2960	3101	2961	45.88	21.34
ν_4	νCH(95)	2960		3095	2956	73.19	6.84
ν_5	νCH(95)	2930		3075	2937	117.41	4.18
ν_6	νCH(94)		2936	3064	2926	60.85	5.93
ν_7	νCH(89)			3051	2914	0.19	0.88
ν_8	νCH(91)			3037	2901	1.28	11.67
ν_9	νCH(90)		2896	3031	2894	95.74	30.21
ν_{10}	νCH(91)			3029	2893	32.30	28.33
ν_{11}	νCH(95)			3028	2891	1.20	0.03
ν_{12}	νCH(92)		2874	3024	2888	0.10	53.14
ν_{13}	νCH(95)	2858		3020	2884	104.49	19.72
ν_{14}	νCH(92)			3012	2877	24.26	3.93
ν_{15}	νCH(87)		2852	3005	2870	0.70	72.98
ν_{16}	νCH(85)			3004	2869	0.07	0.44
ν_{17}	νCH(90)			3001	2866	7.56	3.57
ν_{18}	δHNH(97)	1595		1667	1629	29.51	2.16
		1615					
ν_{19}	δHCH(90)			1517	1482	9.53	0.21
ν_{20}	δHCH(86)			1511	1476	0.23	0.11
ν_{21}	δHCH(90)	1463		1504	1469	1.20	3.62
ν_{22}	δHCH(84)		1453	1503	1468	8.08	5.24
ν_{23}	δHCH(84)			1496	1462	0.51	3.00
ν_{24}	δHCH(92)		1436	1492	1458	0.01	26.18
ν_{25}	δHCH(93)			1490	1456	0.11	1.29
ν_{26}	δHCH(92)			1487	1453	0.28	3.50
ν_{27}	δHCH(91)			1417	1385	1.94	0.46
ν_{28}	δHCH(75)	1380		1407	1374	5.15	0.18
ν_{29}	δHCN(78)			1404	1372	4.86	0.24
ν_{30}	δHCC(67)	1343		1393	1361	3.57	0.26
ν_{31}	δHCN(88)		1361	1388	1356	0.47	3.19
ν_{32}	δHCC(80)	1303		1356	1324	4.24	0.25
ν_{33}	δHCC(82)			1339	1308	0.44	0.07
ν_{34}	δHCC(76)			1335	1304	0.06	1.52
ν_{35}	δHCC(79)		1299	1325	1295	0.18	21.43
ν_{36}	δHCC(62)			1303	1273	0.04	0.06
ν_{37}	δHCC(82)			1302	1272	0.01	0.18
ν_{38}	δHCH(48)			1257	1228	0.02	0.12
ν_{39}	δHCC(84)	1218		1246	1217	2.51	0.08
ν_{40}	δHCC(75)			1213	1185	0.01	0.70
ν_{41}	δCCN(50) + δCCC(25)		1126	1140	1114	0.63	9.16
ν_{42}	νNC(74)	1128	1087	1091	1066	12.41	3.81
ν_{43}	νCC(73)		1073	1070	1045	5.49	8.20
ν_{44}	νCC(73)	1093		1061	1037	7.88	5.32
ν_{45}	δHNC(85)			1061	1037	0.04	0.60
ν_{46}	δCCC(24) + νCC(52)	1072	1035	1049	1025	16.62	3.50
ν_{47}	νCC(81)			1021	997	0.42	1.66
ν_{48}	τHCCH(60)			1001	978	0.49	0.74
ν_{49}	νCC(74)	942		989	966	9.83	0.64
ν_{50}	τHCCC(70)			916	895	0.00	0.03
ν_{51}	δCCN(12) + δCCC(29) + νCC(16)		895	897	877	0.19	7.36
			872				
ν_{52}	δHNH(81)	810	828	830	811	203.93	1.09
ν_{53}	τHCCC(56)			830	810	0.48	0.22
ν_{54}	τHCCH(71)			767	749	0.43	0.01
ν_{55}	δHCC(70)			740	723	0.00	0.01
ν_{56}	τHCCH(86)	724		733	717	4.09	0.01
ν_{57}	δCCN(79)	513		490	479	3.53	0.83
ν_{58}	νCC(19) + δCCC(65)			466	455	0.36	0.11
ν_{59}	δCCN(86)	343		350	341	2.97	1.26
		328					
ν_{60}	τHNCC(78)	254		280	274	49.89	1.53
		277					
ν_{61}	δCCC(89)		281	270	264	0.03	53.31
ν_{62}	τHCCH(80)	230		242	236	0.09	0.14
ν_{63}	τHCCN(91)	187		198	193	1.92	3.54
ν_{64}	τCCCC(89)	176		168	164	0.00	0.13

(*continued on next page*)

Table 3 (*continued*)

Mode	Assignments	Experimental		B3LYP/6-31++G(d,p)			
				Gas Phase			
	PED[a] (⩾10%)	IR	Raman	ν^{b}	ν^{c}	I_{IR} [d]	I_R[d]
ν_{65}	δHCH(10) + τCCCC(63)	139		141	138	1.68	0.00
ν_{66}	τCCCC(84)	122		118	115	0.07	0.71
ν_{67}	τHCNH(93)	80		78	76	0.62	0.00
ν_{68}	τCCCC(86)	69		77	75	1.87	0.51
ν_{69}	τCCCC(94)	56		53	52	0.15	0.00

[a] PED data are taken from VEDA4.
[b] Unscaled wavenumbers.
[c] Scaled with 0.955 above 1800 cm^{-1},0.977 under 1800 cm^{-1}.
[d] I_{IR} and I_R calculated infrared and Raman intensities.

Table 4
Calculated vibrational frequencies (cm^{-1}) for TT form of 1-ha in benzene.

Mode	Assignments	Experimental		B3LYP/6-31++G(d,p)			
				Benzene			
	PED [a] (⩾10%)	IR	Raman	ν^{b}	ν^{c}	I_{IR}[d]	I_R[d]
ν_1	νNH(100)	3371	3385	3575	3414	0.70	10.44
ν_2	νNH(100)	3289	3325	3490	3333	1.55	23.48
ν_3	νCH(98)		2960	3098	2959	56.27	27.45
ν_4	νCH(91)	2960		3093	2954	90.21	9.40
ν_5	νCH(94)	2930		3075	2936	136.41	7.12
ν_6	νCH(90)		2936	3062	2925	99.98	7.75
ν_7	νCH(89)			3050	2913	0.32	1.12
ν_8	νCH(94)			3038	2901	1.65	18.53
ν_9	νCH(95)		2896	3031	2894	95.47	35.23
ν_{10}	νCH(95)			3028	2892	1.21	0.78
ν_{11}	νCH(98)			3028	2891	46.87	51.39
ν_{12}	νCH(96)		2874	3024	2888	0.01	84.23
ν_{13}	νCH(91)	2858		3018	2882	144.67	26.77
ν_{14}	νCH(94)			3012	2876	43.56	4.35
ν_{15}	νCH(92)		2852	3005	2870	1.27	113.69
ν_{16}	νCH(88)			3004	2869	0.22	0.88
ν_{17}	νCH(95)			3002	2866	7.99	0.46
ν_{18}	δHNH(94)	1595 1615		1661	1622	35.93	2.74
ν_{19}	δHCH(92)			1514	1479	11.16	0.21
ν_{20}	δHCH(84)			1508	1473	0.17	0.13
ν_{21}	δHCH(87)	1463		1501	1466	1.31	3.15
ν_{22}	δHCH(81)		1453	1498	1463	9.00	6.88
ν_{23}	δHCH(86)			1493	1459	0.62	0.96
ν_{24}	δHCH(88)		1436	1487	1453	0.23	20.95
ν_{25}	δHCH(95)			1486	1452	0.01	23.15
ν_{26}	δHCH(89)			1483	1449	0.36	4.65
ν_{27}	δHCH(77)			1413	1381	1.94	0.54
ν_{28}	δHCC(72)	1380		1405	1372	4.50	0.24
ν_{29}	δHCH(80)			1403	1371	7.59	0.36
ν_{30}	δHCC(73)	1343		1391	1359	3.22	0.38
ν_{31}	δHNC(90)		1361	1388	1356	0.28	4.55
ν_{32}	δHCC(70)	1303		1354	1323	4.35	0.31
ν_{33}	δHCC(81)			1337	1306	0.34	0.02
ν_{34}	δHCC(78)			1333	1303	0.06	2.56
ν_{35}	δHCC(85)		1299	1325	1294	0.25	30.72
ν_{36}	δHCC(72)			1302	1272	0.03	0.13
ν_{37}	δHCC(77)			1302	1272	0.03	0.27
ν_{38}	δHNC(52) + δHCC(13)			1256	1227	0.03	0.25
ν_{39}	δHCC(82)	1218		1246	1218	2.90	0.08
ν_{40}	δHCH(75)			1211	1183	0.02	1.62
ν_{41}	δCCC(52) + δHCC(17)		1126	1140	1114	0.58	12.32
ν_{42}	νNC(64)	1128	1087	1088	1063	11.24	5.62
ν_{43}	νCC(75)		1073	1069	1045	7.91	10.15
ν_{44}	δHNC(82)	1093		1062	1038	0.06	0.84
ν_{45}	νCC(80)			1061	1037	11.11	8.61
ν_{46}	δCCC(57)	1072	1035	1050	1025	20.03	4.59
ν_{47}	νCC(83)			1020	997	0.59	1.98
ν_{48}	δHCC(65)			1000	977	0.67	0.90
ν_{49}	νCC(74)	942		990	967	13.42	0.63
ν_{50}	τHCCC(62)			916	894	0.00	0.03
ν_{51}	δHCC(42) + δCCC(42)		895 872	897	876	0.49	9.40

Table 4 (*continued*)

Mode	Assignments	Experimental		B3LYP/6-31++G(d,p)			
				Benzene			
	PED [a] (⩾10%)	IR	Raman	ν^{b}	ν^{c}	I_{IR} [d]	I_{R} [d]
ν_{52}	τHCNH(73)	810	828	852	832	220.79	1.58
ν_{53}	τHCCC(56) + τCCCC(11)			829	810	0.60	0.23
ν_{54}	τHCCH(69)			767	749	0.64	0.03
ν_{55}	τHCCH(77)			739	722	0.02	0.00
ν_{56}	τHCCH(90)	724		733	716	5.71	0.01
ν_{57}	δCCN(78)	513		489	478	3.78	0.76
ν_{58}	δCCC(78)			465	455	0.40	0.16
ν_{59}	δCCC(87)	343		349	341	3.39	1.43
		328					
ν_{60}	τHCCC(10) + τHNCC(83)	254					
		277		276	270	61.48	1.33
ν_{61}	δCCC(78)		281	270	264	0.04	60.36
ν_{62}	τHCCH(82)	230		242	236	0.13	0.14
ν_{63}	τHCCN(93)	187		198	193	2.31	3.54
ν_{64}	τCCCC(88)	176		167	163	0.00	0.26
ν_{65}	τCCCC(63)	139		140	137	2.24	0.00
ν_{66}	τCCCC(79)	122		118	115	0.09	1.19
ν_{67}	τHCCC(93)	80		78	76	0.76	0.00
ν_{68}	τCCCC(80)	69		75	73	2.65	0.54
ν_{69}	τCCCC(94)	56		52	51	0.11	0.00

[a] PED data are taken from VEDA4.
[b] Unscaled wavenumbers.
[c] Scaled with 0.955 above 1800 cm^{-1}, 0.977 under 1800 cm^{-1}.
[d] I_{IR} and I_{R} calculated infrared and Raman intensities.

Table 5
Calculated vibrational frequencies (cm^{-1}) for TT form of 1-ha in methanol.

Mode	Assignments	Experimental		B3LYP/6-31++G(d,p)			
				Methanol			
	PED[a] (⩾10%)	IR	Raman	ν^{b}	ν^{c}	I_{IR} [d]	I_{R} [d]
ν_{1}	νNH(100)	3371	3385	3567	3406	1.40	15.49
ν_{2}	νNH(99)	3289	3325	3486	3329	1.07	34.63
ν_{3}	νCH(98)		2960	3095	2956	72.71	36.36
ν_{4}	νCH(92)	2960		3090	2951	115.59	14.81
ν_{5}	νCH(92)	2930		3073	2935	177.17	12.15
ν_{6}	νCH(92)		2936	3059	2922	196.04	11.04
ν_{7}	νCH(90)			3050	2912	0.29	0.90
ν_{8}	νCH(91)			3039	2902	1.31	36.29
ν_{9}	νCH(97)		2896	3029	2893	111.40	58.57
ν_{10}	νCH(92)			3029	2893	0.70	4.54
ν_{11}	νCH(97)			3026	2889	50.39	90.33
ν_{12}	νCH(94)		2874	3024	2888	0.17	151.54
ν_{13}	νCH(93)	2858		3016	2880	199.67	45.67
ν_{14}	νCH(92)			3010	2875	114.57	0.12
ν_{15}	νCH(96)		2852	3006	2870	1.32	171.98
ν_{16}	νCH(94)			3003	2868	0.29	27.07
ν_{17}	νCH(92)			3001	2866	7.73	9.95
ν_{18}	δHNH(91)	1595		1652	1614	47.61	3.33
		1615					
ν_{19}	δHCH(91)			1510	1475	17.02	0.20
ν_{20}	δHCH(90)			1505	1470	0.15	0.27
ν_{21}	δHCH(88)	1463		1497	1463	1.68	2.37
ν_{22}	δHCH(84)		1453	1491	1456	10.23	9.31
ν_{23}	δHCH(88)			1489	1455	0.66	0.14
ν_{24}	δHCH(84)		1436	1482	1448	0.35	6.24
ν_{25}	δHCH(90)			1477	1443	0.66	2.17
ν_{26}	δHCH(96)			1476	1442	0.00	62.43
ν_{27}	δHCH(88)			1408	1376	1.86	0.85
ν_{28}	δHCC(68)	1380		1403	1370	0.96	0.07
ν_{29}	δHCC(77)			1402	1369	13.08	0.95
ν_{30}	δHCC(78)	1343		1388	1356	2.90	0.61
ν_{31}	δHCN(88)		1361	1387	1355	0.04	6.90
ν_{32}	δHCC(80)	1303		1352	1321	4.45	0.40
ν_{33}	δHCC(84)			1334	1303	0.10	0.03
ν_{34}	δHCC(72)			1331	1300	0.06	5.22

(*continued on next page*)

Table 5 (*continued*)

Mode	Assignments	Experimental		B3LYP/6-31++G(d,p)			
				Methanol			
	PED[a] (⩾10%)	IR	Raman	ν^{b}	ν^{c}	I_{IR} [d]	I_{R}[d]
ν_{35}	δHCC(83)		1299	1324	1293	0.36	47.61
ν_{36}	δHCC(72)			1302	1272	0.01	0.30
ν_{37}	δHCH(83)			1301	1271	0.07	0.53
ν_{38}	δHNC(50) + δHCC(14)			1256	1227	0.01	0.67
ν_{39}	δHCC(80)	1218		1247	1218	3.44	0.11
ν_{40}	δHCH(79)			1209	1181	0.05	5.93
ν_{41}	δCCC(55) + δHCC(19)		1126	1140	1113	0.74	17.21
ν_{42}	δCCN(51)	1128	1087	1084	1060	11.24	8.42
ν_{43}	νCC(72)		1073	1069	1044	11.42	12.23
ν_{44}	δHNC(88)	1093		1064	1040	0.10	1.87
ν_{45}	νCC(79)			1061	1037	16.77	15.41
ν_{46}	δCCC(71)	1072	1035	1050	1026	23.32	6.32
ν_{47}	νCC(79)			1019	996	0.78	2.44
ν_{48}	δHCC(58)			1000	977	0.96	1.72
ν_{49}	νCC(67)	942		992	970	19.53	0.85
ν_{50}	τHCCC(71)			915	894	0.01	0.01
ν_{51}	δHCC(36) + δCCC(40)		895 872	896	876	7.47	12.14
ν_{52}	δCCN(15) + τNHCH(66)	810	828	878	858	222.96	2.56
ν_{53}	τHCCC(59)			829	810	0.85	0.44
ν_{54}	τHCCH(78)			767	749	1.12	0.06
ν_{55}	τHCCH(65)			739	722	0.08	0.00
ν_{56}	τHCCH(84)	724		731	714	9.91	0.03
ν_{57}	δCCN(75)	513		488	477	4.06	0.69
ν_{58}	δCCC(68)			465	454	0.47	0.22
ν_{59}	δCCN(87)	343 328		349	341	3.96	1.51
ν_{60}	τHNCC(88)	254 277		281	275	83.07	1.80
ν_{61}	δCCC(64)		281	270	264	0.05	66.68
ν_{62}	τHCCH(76)	230		242	236	0.12	0.28
ν_{63}	τHCCN(92)	187		197	193	2.96	3.16
ν_{64}	τCCCC(92)	176		166	162	0.00	0.53
ν_{65}	τCCCC(71)	139		140	137	2.71	0.00
ν_{66}	τCCCC(83)	122		116	114	0.12	1.46
ν_{67}	τHCCC(93)	80		78	76	1.03	0.50
ν_{68}	τCCCC(80)	69		75	73	3.21	1.07
ν_{69}	τCCCC(89)	56		51	50	0.17	1.09

[a] PED data are taken from VEDA4.
[b] Unscaled wavenumbers.
[c] Scaled with 0.955 above 1800 cm^{-1},0.977 under 1800 cm^{-1}.

GG_6), 3433 cm^{-1} (GG_4, GG_5), and 3338 cm^{-1} (TT, GT), 3341 cm^{-1} (TG, GG_1 and GG_2), 3344 cm^{-1} (GT_1), 3342 cm^{-1} (GG_3, GG_6), 3352 cm^{-1} (GG_4, GG_5), respectively.

CH_3 and CH_2 vibrations

The aliphatic vibrations in the IR spectrum of heptylamine containing structure [16] have been assigned as follows: asymmetric stretching vibration of CH_3: 2956 cm^{-1}, asymmetric stretching vibration of CH_2: 2927–2930 cm^{-1} and symmetric stretching vibration of CH_2: 2872 cm^{-1}. CH_3 antisymmetric stretching of 1-ha is observed at 2960 cm^{-1} (both IR and R). The theoretically calculated values for this mode in the gas phase are between 2955 and 2966 cm^{-1}. CH_2 antisymmetric stretching modes are observed at 2936 cm^{-1} (R) and 2930 cm^{-1} (IR). This mode has been calculated in the range 2944–2920 cm^{-1}. Based on the mole fractions of the conformers of 1-ha, the band which appears at 2896 cm^{-1} (R) could be attributed to a combination of $\nu_s(CH_3)$ and $\nu_s(CH_2)$. Furthermore, the bands appear at 2874 cm^{-1} (R), 2858 cm^{-1} (IR) and 2852 cm^{-1} (R) due to symmetric stretching vibrations of CH_2. The corresponding scaled theoretical values of these modes are between 2890 and 2869 cm^{-1}. In the high wavenumber region of the spectra, the anharmonicity can explain substantial differences between the experimental and calculated values. Alternatively, these differences may be due to intra/inter-molecular interactions or to the laser used for Raman.

Other vibrations

The N–H bending mode in IR spectra of heptylamine containing structures has been observed in the range 1597–1632 cm^{-1} [4,5,7]. While $\delta(NH_2)$ scissoring of 1-ha seems Raman inactive or its intensity is too low to identify, its IR band appears at 1595 and 1615 cm^{-1} which is theoretically calculated as 1629 cm^{-1} (TT, GT), 1624 cm^{-1} (TG), 1628 cm^{-1} (GT_1), 1625 cm^{-1} (GG_1, GG_2, GG_4 and GG_5) and 1623 cm^{-1} (GG_3 and GG_6). The typical overlap of the CH_3 asymmetric bending and CH_2 scissoring vibrations was previously reported between 1459 and 1466 cm^{-1} [16]. The bands at 1463 cm^{-1} (IR), 1453 and 1436 cm^{-1} (R) may be assigned as $\delta_a(CH_3)$ and $\delta(CH_2)$, respectively.

The CC or CN stretching and HCH, HCN, HCC, CCN or CCC bending modes dominate the regions of 1400–1000 cm^{-1} while HCC, HCH, HNH, CCC or CCN bending and HCCC, HCCH, HCNH, HCCN or CCCC torsion modes are seen in the low frequency region (1000–50 cm^{-1}). Similar situations have been shown in calculations. Vibrational modes in the low wavenumber region of the spectrum contain contributions of several internal coordinates

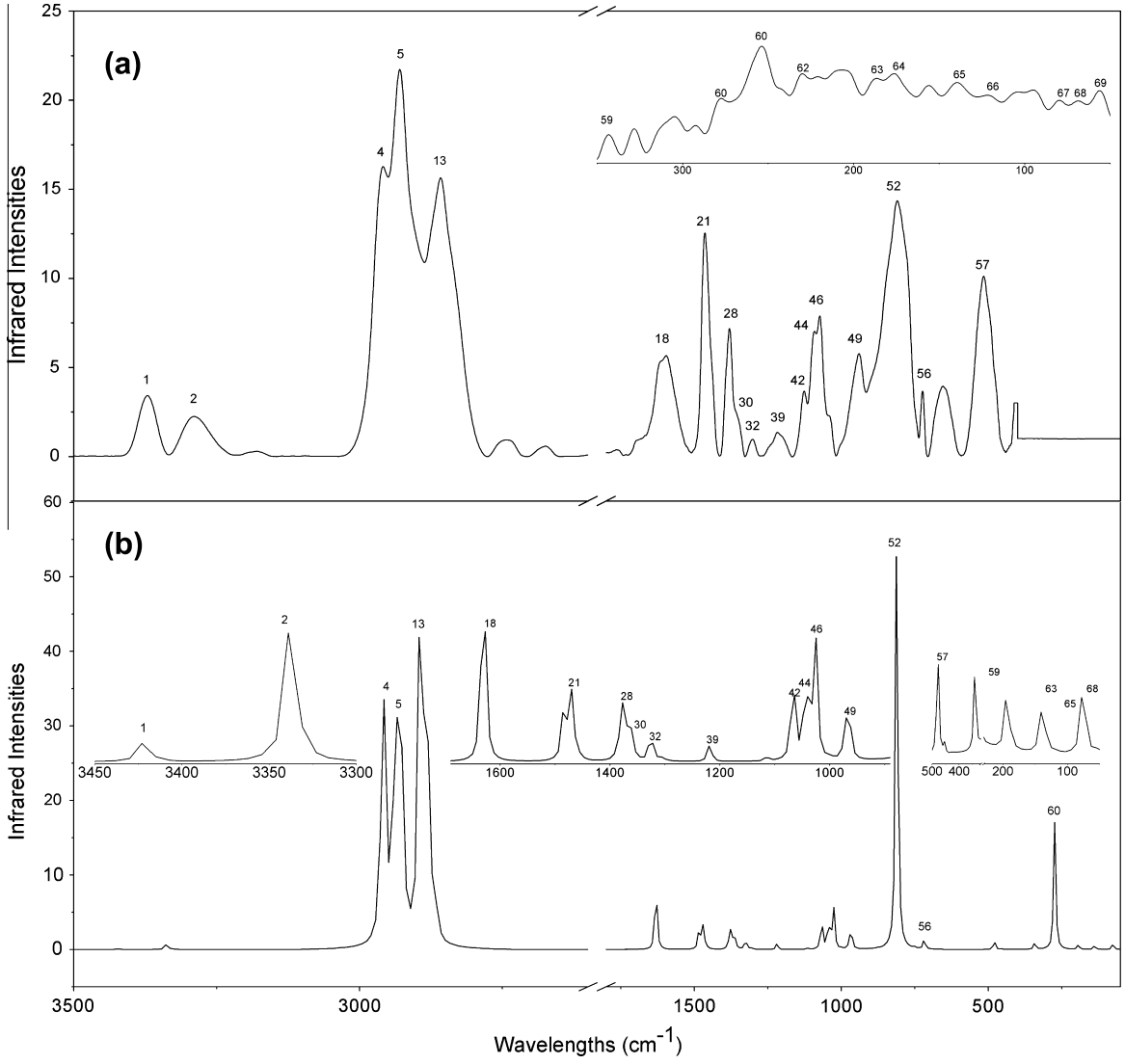

Fig. 2. Experimental (a) and theoretical (b) IR spectra for TT isomer of 1-ha.

and their assignment is a reduction approximation to one of two of the internal coordinates.

Solvent effect on frequencies and intensities

As can be seen from Tables 3–5, if the vibrational assignments are investigated one-by-one, the assignments in various medium are generally consistent with one another. As the presence of dielectric medium has a strong influence on the vibrational frequencies, there are significant changes in the presented theoretical vibrational values. Some important vibrational motions are here described. The NH bond lengths increase on going from the gas phase to the solvent phase. Therefore, the NH stretching frequencies should decrease. It is clearly observed in Tables 3–5 that these requirements are substantially fulfilled for 1-ha. These frequencies shifts are explained in terms of increased positive character on nitrogen atom in solvents of high dielectric constant and, the amount of hydrogen bonding [43].

Regarding the calculated fundamentals, the computed vibrational intensities in the gas phase are in reasonable agreement with the experimental results in both high and low frequency regions. It is important to note that calculations have been performed for a single molecule in the gaseous state, contrary to the experimental values recorded in the presence of intermolecular interactions. IR intensities are expected to dramatically change when the solute is solvated and this is indeed the case in our present study. As can be seen from Tables 3–5, Tables S1–6, Figs. 4 and S1, the noticeable changes are shown in many modes and the calculated intensities in solutions are very high when compared to those in the gas phase for most cases. Like IR intensities, significant changes in Raman intensities are seen when the molecule is solvated. For the IR and Raman intensities, the increases in methanol are larger than in benzene. On the other hand, frontier molecular orbital energy and energy gap of all conformations in various medium is also given as Supplementary material (Table S8 and Fig. S1).

Conclusion

The experimental and theoretical vibrational investigations of 1-ha are successfully performed by using FT-IR, Raman and quantum chemical calculations. In conclusion, the following results can be summarized:

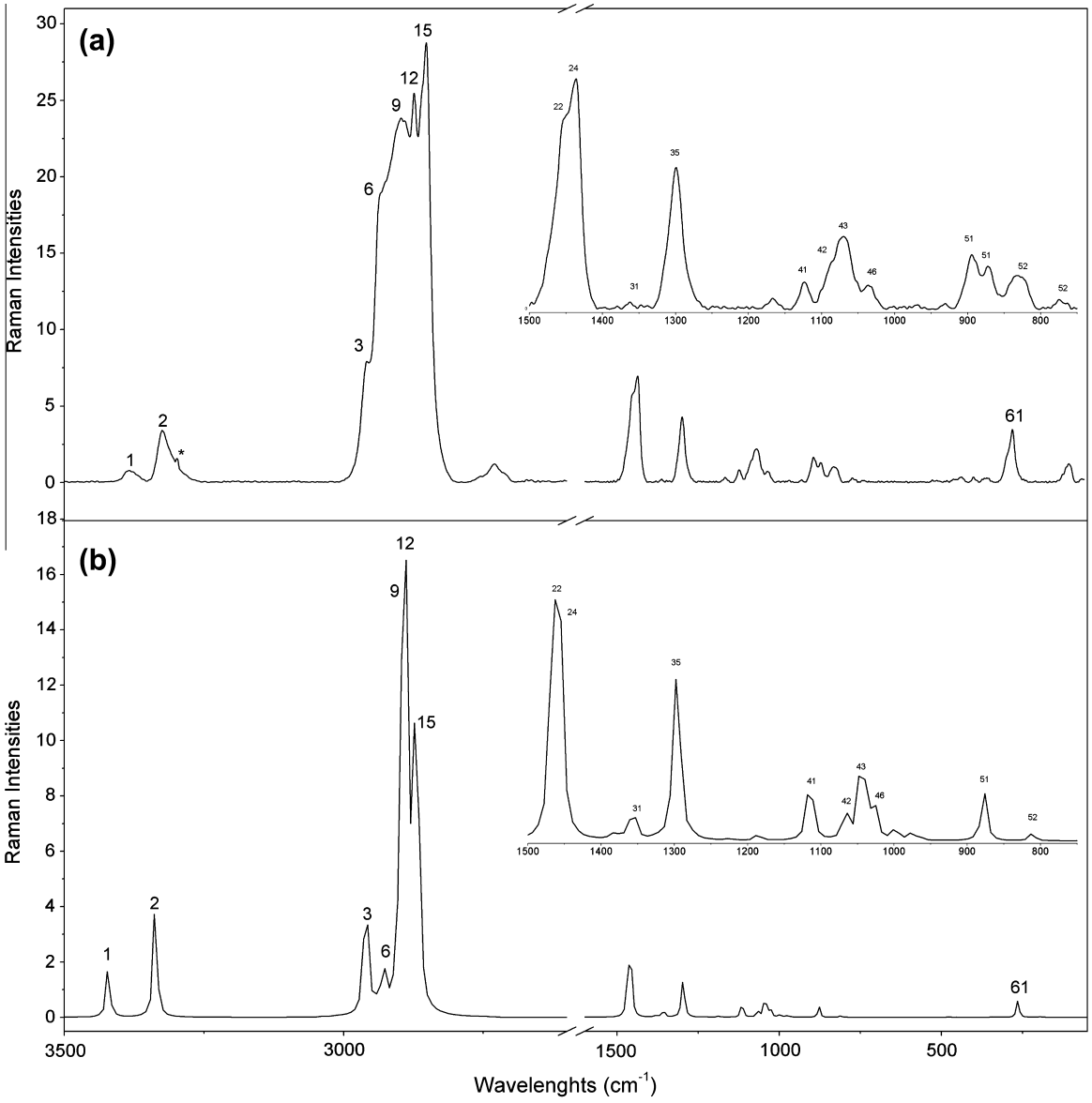

Fig. 3. Experimental (a) and theoretical (b) Raman spectra for TT isomer of 1-ha.

1. Results of energy calculations for gas phase and solvations show that the TT form is the most stable isomer of 1-ha and there are low interconversion energy barriers. These results also indicated that the 1-ha molecule contains several energetically and so the geometrically possible conformers at the same time at room temperature. Furthermore, the conformational energy barrier is independent of the solvent. However, the minimum energies of the optimized structures decrease, or 1-ha tends to be more stable, as the polarity of the solvents increases.
2. The following (IR/Raman) mean absolute deviations (MAD) between the experimental and calculated frequencies are found for gas phase: 18.00/14.03 cm^{-1} (TT), 17.68/14.69 cm^{-1} (TG), 20.89/14.58 cm^{-1} (GT), 22.71/13.92 cm^{-1} (GT_1), 20.18/13.92 cm^{-1} (GG_1), 20.39/13.75 cm^{-1} (GG_2), 20.50/15.14 cm^{-1} (GG_3), 22.61/15.69 cm^{-1} (GG_4), 22.57/15.75 cm^{-1} (GG_5) and 20.54/15.08 cm^{-1} (GG_6). Also, the correlation values (IR/Raman) for the gas phase are found to be 0.99948/0.99983 (TT), 0.99951/0.99974 (TG), 0.999936/0.99984 (GT), 0.99932/0.99980 (GT_1), 0.99950/0.99980 (GG_1), 0.99947/0.99979 (GG_2), 0.99942/0.99975 (GG_3, GG_6) and 0.99932/0.99973 (GG_4, GG_5). It can be seen that the B3LYP/6-31++G(d,p) calculation is reliable and makes the understanding of vibrational spectra of 1-ha easier. The MAD and R^2 values of all conformations for benzene and methanol medium are also given as Supplementary material (Table S7).
3. Some significant changes are found in the geometric parameters when 1-ha in solvated.
4. From lower to higher dielectric, the dipole moment increases and there are very significant changes in vibrational frequencies and assignments due to dielectric medium. In general, the frequency differences increase when going from non-polar to polar solvents.
5. Solvent effects on vibrational intensities are also considerable and they increase as one goes from lower to higher dielectric constant in the most cases.
6. Any differences observed between the experimental and calculated values may be due to the fact that the calculations have been performed for a single molecule in the gas and solvations

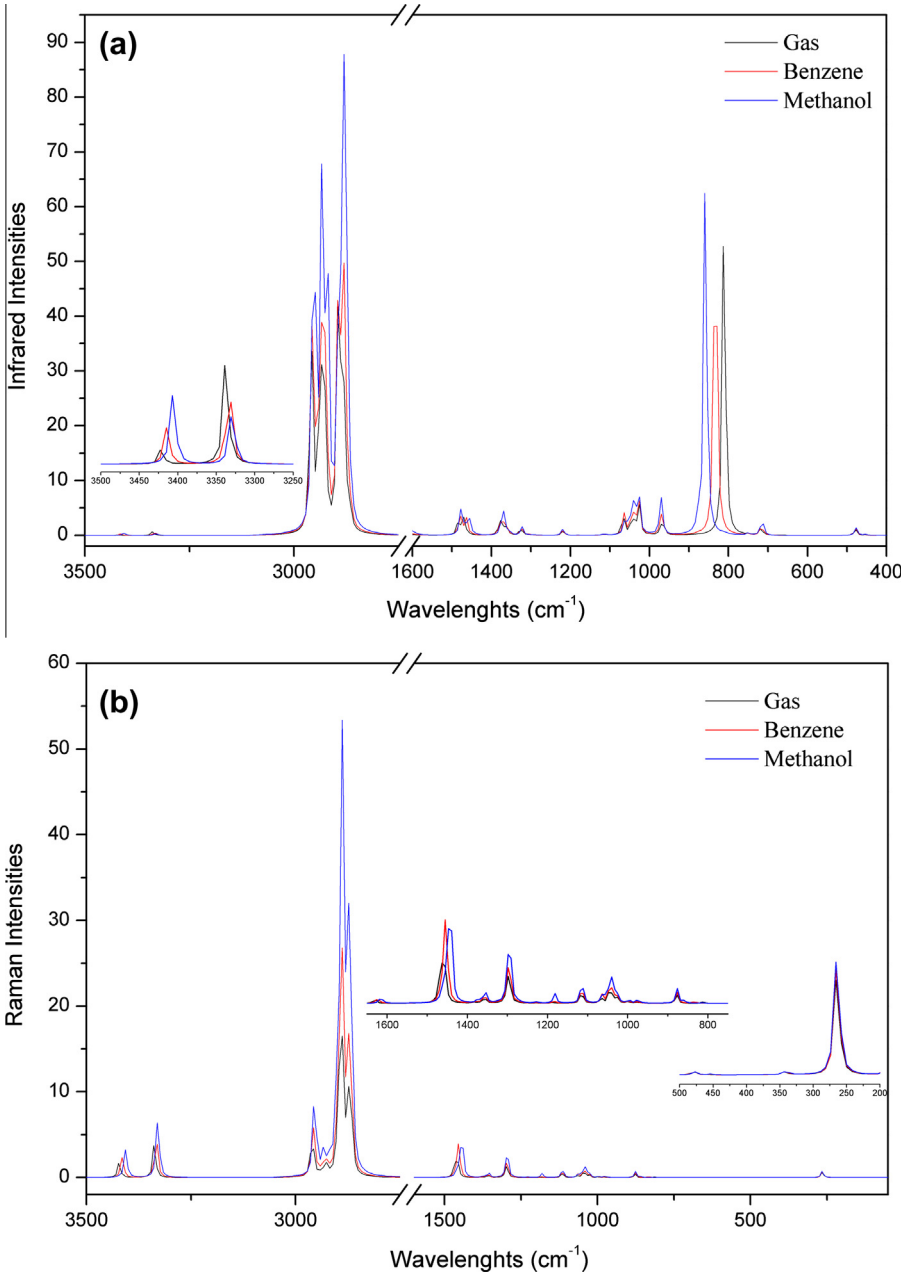

Fig. 4. Theoretical IR (a) and Raman (b) spectra for TT isomer of 1-ha in various medium.

states, whereas the experimental values in the liquid phase have been recorded in the presence of intermolecular interactions.

Acknowledgements

We are deeply grateful to Taryn Nash for editing of the manuscript and to Mehmet Fatih Kaya for the VEDA 4 program.

Appendix A. Supplementary material

Supplementary data associated with this article can be found, in the online version, at http://dx.doi.org/10.1016/j.saa.2013.05.097.

References

[1] K.M. McLean, S.L. McArthur, R.C. Chatelier, P. Kingshott, H.J. Griesser, Colloid Surface B 17 (2000) 23–35.
[2] P. Nava, M. Cecchini, S. Chirico, H. Gordon, S. Morley, D. Manorb, J. Atkinson, Bioorgan. Med. Chem. 14 (2006) 3721–3736.
[3] A. Seki, F. Ishiwata, Y. Takizawa, M. Asami, Tetrahedron 60 (2004) 5001–5011.
[4] C.M. M'thiruaine, H.B. Friedrich, E.O. Changamu, M.D. Bala, Inorg. Chim. Acta 366 (2011) 105–115.
[5] C.M. M'thiruaine, H.B. Friedrich, E.O. Changamu, M.D. Bala, Inorg. Chim. Acta 382 (2012) 27–34.
[6] A.R. Khomutov, A.R. Simonyan, J. Vepsalainen, T.A. Keinanen, L. Alhonen, J. Janne, Russ. J. Bioorg. Chem. 31 (2005) 189–195.
[7] R. Zeng, X. Fu, Y. Sui, X. Yang, M. Sun, J. Chen, J. Organomet. Chem. 693 (2008) 2666–2672.
[8] S. Chandrasekhar, T. Ramachandar, B.V. Rao, Tetrahedron Asymmetry 12 (2001) 2315–2321.
[9] I.G. Binev, Y.I. Binev, B.A. Stamboliyska, I.N. Juchnovski, J. Mol. Struct. 435 (1997) 235–245.
[10] M.K. Nayak, J. Photochem. Photobiol. A 217 (2011) 40–48.

[11] M. Aslam, L. Fu, S. Li, V.P. Dravid, J. Colloid Interface Sci. 290 (2005) 444–449.
[12] P. Koegler, A. Clayton, H. Thissen, G.N.C. Santos, P. Kingshott, Adv. Drug Deliver Rev. 64 (2012) 1820–1839.
[13] F. Gosetti, E. Mazzucco, M.C. Gennaro, E. Marengo, Anal. Bioanal. Chem. 405 (2013) 907–916.
[14] N.V. Kuzmina, F.F. Khizbullin, T.Ya. Gadomskii, V.N. Maistrenko, J. Anal. Chem. 63 (2008) 664–667.
[15] M. Raoux, N. Azorin, C. Colomban, S. Rivoire, T. Merrot, P. Delmas, M. Crest, Toxicol. in Vitro 27 (2013) 402–408.
[16] J. Paivarinta, S. Karlsson, A. Poso, M. Hotokka, Chem. Phys. 263 (2001) 127–138.
[17] J. Paivarinta, S. Karlsson, M. Hotokka, A. Poso, Chem. Phys. Lett. 327 (2000) 420–424.
[18] J.A. Abys, S. Sun, T. Antonellis, US Patent, 0175022 A1, 2012.
[19] X.C. Zhou, S.C. Nga, H.S.O. Ghana, S.F.Y. Lib, Anal. Chim. Acta 345 (1997) 29–35.
[20] X. Ye, L. Qi, Nano Today 6 (2011) 608–631.
[21] P.G. Hartley, S.L. McArthur, K.M. McLean, H.J. Griesser, Langmuir 18 (2002) 2483–2494.
[22] K. Vasilev, L. Britcher, A. Casanal, H.J. Griesser, J. Phys. Chem. B 112 (2008) 10915–10921.
[23] H. Chen, A. Roy, J.B. Baek, L. Zhu, J. Qua, L. Dai, Mater. Sci. Eng. Rep. 70 (2010) 63–91.
[24] M. Wimmerova, L. Macholan, Biosens. Bioelectron. 14 (1999) 695–702.
[25] G. Rauhut, P. Pulay, J. Phys. Chem. 99 (1995) 3093–3100.
[26] A.P. Scott, L. Radom, J. Phys. Chem. 100 (1996) 16502–16513.
[27] S.S. Panikar, G.A. Guirgis, T.G. Sheehan, D.T. Durig, J.R. Durig, Spectrochim. Acta A 90 (2012) 118–124.
[28] C. Parlak, J. Mol. Struct. 966 (2010) 1.–7.
[29] Ö. Alver, C. Parlak, J. Mol. Struct. 975 (2010) 85–92.
[30] Ö. Alver, C. Parlak, J. Theory Comput. Chem. 9 (2010) 667–685.
[31] Ö. Alver, C. Parlak, Vib. Spectrosc. 54 (2010) 1–9.
[32] E. Güneş, C. Parlak, Spectrochim. Acta A 82 (2011) 504–512.
[33] M.J. Frisch, G.W. Trucks, H.B. Schlegel, G.E. Scuseria, M.A. Robb, J.R. Cheeseman, G. Scalmani, V. Barone, B. Mennucci, G.A. Petersson, H. Nakatsuji, M. Caricato, X. Li, H.P. Hratchian, A.F. Izmaylov, J. Bloino, G. Zheng, J.L. Sonnenberg, M. Hada, M. Ehara, K. Toyota, R. Fukuda, J. Hasegawa, M. Ishida, T. Nakajima, Y. Honda, O. Kitao, H. Nakai, T. Vreven, J.A. Montgomery, Jr., J.E. Peralta, F. Ogliaro, M. Bearpark, J.J. Heyd, E. Brothers, K.N. Kudin, V.N. Staroverov, R. Kobayashi, J. Normand, K. Raghavachari, A. Rendell, J.C. Burant, S.S. Iyengar, J. Tomasi, M. Cossi, N. Rega, J.M. Millam, M. Klene, J.E. Knox, J.B. Cross, V. Bakken, C. Adamo, J. Jaramillo, R. Gomperts, R.E. Stratmann, O. Yazyev, A.J. Austin, R. Cammi, C. Pomelli, J.W. Ochterski, R.L. Martin, K. Morokuma, V.G. Zakrzewski, G.A. Voth, P. Salvador, J.J. Dannenberg, S. Dapprich, A.D. Daniels, Ö. Farkas, J.B. Foresman, J.V. Ortiz, J. Cioslowski, D.J. Fox, Gaussian 09, Revision A.1, Gaussian Inc., Wallingford CT, 2009.
[34] R.D. Dennington, T.A. Keith, J.M. Millam, GaussView 5.0.8, Gaussian Inc., 2008.
[35] J.R. Durig, W.B. Beshir, S.E. Godbey, T.J. Hizer, J. Raman Spectrosc. 20 (1989) 311–333.
[36] H.D. Stidham, J.R. Durig, Spectrochim. Acta A 42 (1986) 105–111.
[37] M.H. Jamróz, Vibrational energy distribution analysis: VEDA 4 program, Warsaw, 2004.
[38] G. Keresztury, S. Holly, J. Varga, G. Besenyei, A.Y. Wang, J.R. Durig, Spectrochim. Acta A 49 (1993) 2007–2026.
[39] A. Asadi, B.O. Patrick, D.M. Perin, J. Org. Chem. 72 (2007) 466–475.
[40] G.J. Reiss, Acta Cryst. E 67 (2011) 2684–2685.
[41] T. Tran, T.B. Malloy Jr., J. Mol. Struct. 970 (2010) 66–74.
[42] H. Tavakol, J. Mol. Struct. Theochem. 916 (2009) 172–179.
[43] G. Socrates, Infrared and Raman Characteristic Group Frequencies, third ed., John Wiley & Sons Ltd., England, 2001.